TI Designs

Low-Power Door and Window Sensor With Sub-1GHz and 10-Year Coin Cell Battery Life Reference Design

👏 **TEXAS INSTRUMENTS**

Overview

This TI Design uses Texas Instruments' ultra-low-power consumption digital Hall effect sensors and the SimpleLink™ ultra-low-power sub-1GHz wireless microcontroller (MCU) platform to demonstrate a door and window sensor with extremely long battery life and no wiring required.

Resources

TIDA-01066	Design Folder
CC1310	Product Folder
DRV5032	Product Folder
LAUNCHXL-CC1310	Product Folder
TI-15.4-STACK	Tool Folder

TI E2E™ Community

ASK Our E2E Experts

Features

- Ultra-Low-Power Design Resulting in 10-Year Battery Life From Single CR2032 Coin Cell
- Magnetic Field Sensing Always Powered On To Enable Continuous Monitoring
- Detects Cylindrical Neodymium Magnet Up To 20 mm (0.787 in)
- Dual-Sensor Architecture Detects Tampering Magnet
- IEEE 802.15.4e/g Stack with Collector and Sensor Application
- Designed For SimpleLink Sub-1GHz Wireless Connectivity LaunchPad™ (LAUNCHXL-CC1310)

Applications

- Door and Window Sensor
- Magnetic Contact Switch
- Battery Powered Applications
- Building Automation
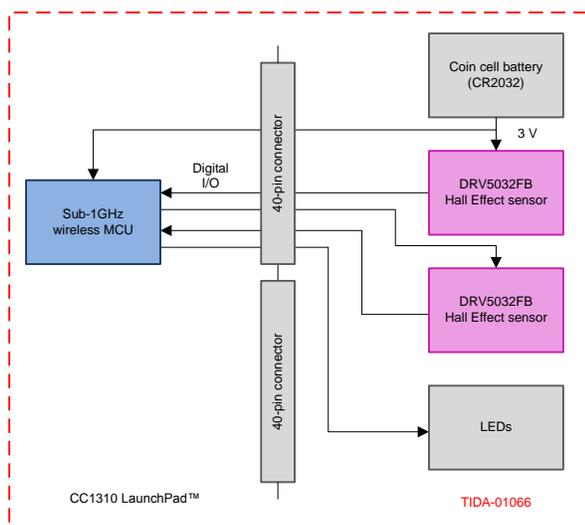
Copyright © 2016, Texas Instruments Incorporated

⚖ An IMPORTANT NOTICE at the end of this TI reference design addresses authorized use, intellectual property matters and other important disclaimers and information.

1 System Overview

1.1 System Description

Many industrial and building automation security systems use sensors to monitor when doors and windows are opened and closed. In the security system a central monitoring device generates notifications and alarms based on the information from multiple door and window sensors. These systems require increasing numbers of wireless sensor nodes to reduce installation costs and to make the systems more flexible for future expansion by eliminating wiring. However, one of the major limitations for a large wireless network is power. Because the sensors are battery powered, the maintenance cost associated with periodic battery replacement can become prohibitive. Depending on the power consumption and battery configuration, typical battery powered door and window sensors can run anywhere from four to eight years before the batteries need to be replaced.

Magnets are commonly used in window and door sensor applications to determine when a window or door is opened or closed. In a typical configuration the magnet is embedded in the window or door and the sensor is attached to the window or door frame. The sensor and magnet are placed such that they are in close proximity when the door or window is closed, and away from each other when the window or door is opened.

Because these sensors are used primarily in security applications, a feature is needed to detect so-called tampering magnets, which can be used to trick the sensor into thinking the door or window is closed. Configurations using multiple sensors can be used to detect tampering magnets.

Enabled by Texas Instruments' ultra-low-power digital Hall effect sensors and the SimpleLink ultra-low-power wireless MCU platform, the Low-Power Door and Window Sensor With Sub-1GHz and 10-Year Coin Cell Battery Life Reference Design demonstrates a door and window sensor solution requiring no wiring while also fully maximizing the battery life.

At a high level, this TI Design consists of a CR2032 coin cell battery, two ultra-low-power digital Hall effect sensors, and an ultra-low-power wireless MCU. The Hall effect sensors drive their outputs low when the magnetic flux density from a nearby magnet exceeds their operating point threshold, and drive their pin high when the magnetic flux density decreases to less than their release point threshold. The digital outputs of the Hall effect sensors serve as interrupts to the wireless MCU so that the MCU can operate in its lowest power sleep mode during times where there is no change in the magnetic flux density and only wakes up to send messages back to a remote host when a change has been detected. The IEEE 802.15.4e/g Stack from TI is used to send messages back to a central node using a wireless network. Due to the ultra-low-power consumption design of the entire system, this TI Design achieves a 10-year battery life from a single CR2032 coin cell battery.

This design guide addresses component selection, design theory, and the testing results of this TI Design system. The scope of this design guide gives system designers a head-start in integrating TI's ultra-low power consumption digital Hall effect sensors and the SimpleLink ultra-low-power wireless MCU platform.

The following subsections describe the various blocks within the TI Design system and what characteristics are most critical to best implement the corresponding function.

1.1.1 Hall Effect Sensors

In this TI Design, a digital Hall effect sensor is used to detect a magnet embedded in a door or window frame, and a second digital Hall effect sensor is used to detect a tampering magnet. In door and window sensor applications, it is important to maximize the distance between the sensor and magnet to give the end-user flexibility during installation of the final product. Average power consumption is also important because these systems are battery-operated and must remain operational for several years before replacing the battery.

The DRV5032 digital Hall effect sensor from Texas Instruments is ideally suited to meet the distance and power requirements of a door and window sensor application. Specifically, the DRV5032FB magnetic threshold operating point, B_{OP}, of 3.1 mT allows it to detect magnets up to 20 mm (see Section Section 4.1.2). Also, the power consumption of the DRV5032FB is extremely low, averaging 0.57 µA at 3 V with a sampling frequency of 5 Hz. Furthermore, the omnipolar response of the DRV5032FB allows it to detect either the north or south pole of the magnet, greatly simplifying assembly. Finally, interfacing to the device is straightforward with any MCU platform using a single general-purpose input/output (I/O) pin.

This TI Design uses one DRV5032FB digital Hall effect sensor to detect the primary magnet and a second DRV5032FB sensor to detect a tampering magnet. The two sensors are located far enough apart from each other such that the second sensor is not activated by the primary magnet and instead only activates when a tampering magnet is in close proximity.

Provisions for installing other DRV5032 devices with different sensitivities are also included in this TI Design. For example, the DRV5032AJ device has lower sensitivity (higher B_{OP}) and can be placed closer to the main sensor while at the same time be used to detect tampering magnets. An unpopulated resistor pad is included in the design for devices with an open-drain output that require a pull-up resistor. The Hall effect sensor can also be powered directly from the MCU I/O pin such that a duty-cycled power design can be implemented to further reduce average power consumption and increase battery life.

1.1.2 Ultra-Low-Power MCU

In this TI Design, transmitting the sensor information to some central location for processing is necessary. However, because power consumption is always a concern in battery-based applications, the radio and processor must be low power. Also, the wireless protocol required for the end-equipment system is an important consideration for the selection of the radio device.

A TI's SimpleLink ultra-low-power wireless MCU platform, with a combined radio and MCU enables an extremely long battery life for sensor end-nodes. Furthermore, the CC1310 is a multi-standard device with software stack support for wM-Bus and IEEE 802.15.4g. This TI Design uses TI's SimpleLink TI-15.4 Stack to interface to a star network, but the hardware as built can work with other protocols as well.

1.1.3 Coin Cell Battery

The power source for this TI Design is a CR2032 lithium-ion coin cell. The selection of the CR2032 coin cell battery as the power source was due to the ubiquity of that battery type, particularly in small form factor systems such as a sensor end-node.

The voltage characteristics of a lithium-ion CR2032 coin cell battery are also ideal. The output voltage remains relatively flat throughout the discharge life until the cell is nearly depleted. When the cell is depleted, the output voltage drops off relatively quickly.

The temperature characteristics of lithium-ion batteries are also superior to that of alkaline cells, particularly at lower temperatures. This superiority is due to lithium-ion cells having a non-aqueous electrolyte that performs better than aqueous electrolytes commonly found in alkaline batteries. However, the CR2032 coin cell battery is the limiting component in terms of the operating temperature range; all of the integrated circuits and other electrical components are specified to operate at a wider temperature range than the battery. Therefore, the specified operating temperature range of the TI Design system is 0°C to 50°C. Given an appropriate weather-proof enclosure, this TI Design system is suited for both indoor and outdoor use.

Immediately following the battery are two low R_{DS_ON} P-channel MOSFETs and a bulk capacitor. The P-channel MOSFETs prevents damage to the hardware if the coin cell battery is inserted backwards while minimizing the forward voltage drop in normal operation. The bulk capacitor is sized to prevent too much voltage droop, particularly during the transitions into the MCU on-state for radio transmissions.

1.2 Key System Specifications

Table 1. Key System Specifications

PARAMETER	SPECIFICATIONS	DETAILS
Input power source	CR2032 Lithium-ion coin cell battery (3.0-V nominal voltage)	Section 2.2
Sensor type	Hall effect	Section 1.1.1
Average standby-state current consumption	1.97 µA	Section 4.2.1
Estimated battery life	> 10 years	Section 4.2.1.1
Magnet sensing distance	20 mm [1]	Section 4.2.2
Sensor sampling frequency	5 Hz	Section 1.1.1
Transmitter frequency	915 MHz	Section 2.3
Network type	Star	Section 1.1.2
Radio transmission range	~60 meters	Section 4.2.3
Operating conditions	0°C to 50°C	Section 1.1.3
Form factor	34-mm×53-mm rectangular PCB	Section 5.3

[1] ¼" diameter × 7/8" length Neodymium-N42 magnet

1.3 Block Diagram
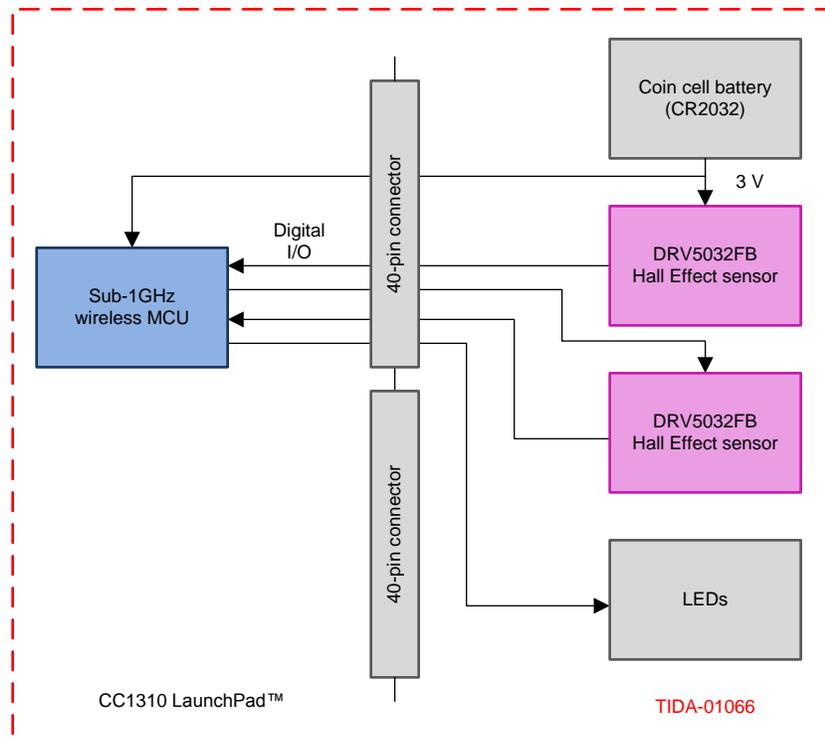
Copyright © 2016, Texas Instruments Incorporated

Figure 1. Block Diagram

1.4 Highlighted Products

This TI Design features the following devices:

- DRV5032 (Section 1.4.1): ultra-low power digital-switch Hall effect sensor
- CC1310 (Section 1.4.2): SimpleLink multi-standard sub-1GHz ultra-low-power wireless MCU

For more information on each of these devices, see their respective product folders at www.ti.com.

1.4.1 DRV5032

The DRV5032 is an ultra-low-power digital switch Hall effect sensor, designed for the most compact and battery-sensitive systems. The device is offered in multiple magnetic sensitivities, sampling rates, output drivers, and packages to accommodate various applications.

When the applied magnetic flux density exceeds the B_{OP} threshold, a device output drives a low voltage. The output stays low until the flux density decreases to less than B_{RP}, and then the output either becomes high-impedance or drives a high voltage, depending on the device version. By incorporating an internal oscillator, the DRV5032 samples the magnetic field and updates the output at a rate of 20 Hz, or 5 Hz for the lowest current consumption. Both omnipolar and unipolar magnetic responses are available.

The DRV5032 operates from a V_{CC} range of 1.65 to 5.5 V, and is packaged in a SOT-23 and small SON.

Features:

- Industry-leading ultra-low power consumption
  - 5 Hz version: 0.4 µA with 1.8 V
  - 20 Hz versions: 1.3 µA with 3 V
- 1.65- to 5.5-V operating V_{CC} range
- Magnetic threshold options (typical B_{OP}):
  - 3.1 mT — high sensitivity
  - 7.5 mT — medium sensitivity
  - 50 mT — low sensitivity
- Omnipolar or unipolar magnetic response
- 20-Hz and 5-Hz sample rate options
- Push-pull output driver and open-drain options
- SOT-23 or small SON package
- –40°C to 85°C operating temperature range

1.4.2 CC1310

The CC1310 is a member of the CC26xx and CC13xx family of cost-effective, ultra-low-power, 2.4-GHz and Sub-1 GHz RF devices. Very low active RF and microcontroller (MCU) current consumption, in addition to flexible low-power modes, provide excellent battery lifetime and allow long-range operation on small coin-cell batteries and in energy-harvesting applications. The CC1310 device is the first device in a Sub-1 GHz family of cost-effective, ultra-low-power wireless MCUs. The CC1310 device combines a flexible, very low power RF transceiver with a powerful 48-MHz Cortex-M3 microcontroller in a platform supporting multiple physical layers and RF standards. A dedicated Radio Controller (Cortex-M0) handles low-level RF protocol commands that are stored in ROM or RAM, thus ensuring ultra-low power and flexibility. The low-power consumption of the CC1310 device does not come at the expense of RF performance; the CC1310 device has excellent sensitivity and robustness (selectivity and blocking) performance.

The CC1310 device is a highly integrated, true single-chip solution incorporating a complete RF system and an on-chip DC-DC converter.

Sensors can be handled in a very low-power manner by a dedicated autonomous ultra-low-power MCU that can be configured to handle analog and digital sensors; thus the main MCU (Cortex-M3) can maximize sleep time.

The CC1310 power and clock management and radio systems require specific configuration and handling by software to operate correctly, which has been implemented in the TI-RTOS. TI recommends using this software framework for all application development on the device. The complete TI-RTOS and device drivers are offered in source code free of charge.

Features:
- Microcontroller
  - Powerful ARM® Cortex®-M3
  - EEMBC CoreMark® score: 142
  - EEMBC ULPBench™ score: 158
  - Clock speed up to 48 MHz
  - 128KB of in-system programmable flash
  - 8KB of SRAM for cache
    (or as General-Purpose RAM)
  - 20KB of ultra-low-leakage SRAM
  - 2-Pin cJTAG and JTAG debugging
  - Supports over-the-air (OTA) update
- Ultra-low-power sensor controller
  - Can run autonomously from the rest of the system
  - 16-bit architecture
  - 2KB of ultra-low-leakage SRAM for code and data
- Efficient code-size architecture, placing parts of
  TI-RTOS, drivers, and bootloader in ROM
- RoHS-compliant package
  - 7-mm × 7-mm RGZ VQFN48 (30 GPIOs)
  - 5-mm × 5-mm RHB VQFN32 (15 GPIOs)
  - 4-mm × 4-mm RSM VQFN32 (10 GPIOs)
- Peripherals
  - All digital peripheral pins can be routed to any GPIO
- Four general-purpose timer modules (Eight 16-bit or four 32-bit timers, PWM each)
  - 12-bit ADC, 200 ksamples/s, 8-channel analog MUX
  - Continuous time comparator
  - Ultra-low-power clocked comparator
  - Programmable current source
  - UART
  - 2× SSI (SPI, MICROWIRE, TI)
  - I²C, I2S
  - Real-time clock (RTC)
  - AES-128 security module
  - True random number generator (TRNG)
  - Support for eight capacitive sensing buttons
  - Integrated temperature sensor
- External system
  - On-chip internal DC-DC converter
  - Seamless integration with the SimpleLink™ CC1190 range extender
- Low power
  - Wide supply voltage range: 1.8 to 3.8 V
  - Active-mode MCU 48-MHz running Coremark: 2.5 mA (51 µA/MHz)
  - Active-mode MCU: 48.5 CoreMark/mA
 - Active-mode sensor controller at 24 MHz: 0.4 mA + 8.2 µA/MHz

- – Sensor controller, one wakeup every second performing one 12-bit ADC sampling: 0.95 µA
- – Standby: 0.7 µA (RTC running and RAM and CPU retention)
- – Shutdown: 185 nA (wakeup on external events)
- RF section
  - – Excellent receiver sensitivity –124 dBm using long-range mode, –110 dBm at 50 kbps (sub-1 GHz)
  - – Excellent selectivity (±100 kHz): 56 dB
  - – Excellent blocking performance (±10 MHz): 90 dB
  - – Programmable output power up to 14 dBm
  - – Single-ended or differential RF interface
  - – Suitable for systems targeting compliance with worldwide radio frequency regulations
    - • ETSI EN 300 220, EN 303 204 (Europe)
    - • FCC CFR47 Part 15 (US)
    - • ARIB STD-T108 (Japan)
  - – Wireless M-Bus and selected IEEE 802.15.4g PHY
- Tools and development environment
  - – Full-feature and low-cost development kits
  - – Multiple reference designs for different RF configurations
  - – Packet sniffer PC software
  - – Sensor Controller Studio
  - – SmartRF™ Studio
  - – SmartRF Flash Programmer 2
  - – IAR Embedded Workbench® for ARM
  - – Code Composer Studio™

2   System Design Theory

The Low-Power Door and Window Sensor With Sub-1GHz and 10-Year Coin Cell Battery Life Reference Design senses the presence or absence of a magnetic field within the range of the Hall effect sensor. A second Hall effect sensor is used to detect the magnetic field of a tampering magnet. Each Hall effect sensor outputs a digital signal, which can be used as an interrupt to the wireless MCU to save power by only waking the MCU when it is needed. The following sections discuss the details of the design for the different circuit sections that make up the design's overall subsystem.

2.1   Sensor Selection

Reed switches and Hall effect sensors are two technologies used to detect the presence (or absence) of a magnet embedded in a door or window frame. Reed switches use a physical switch that closes in the presence of a magnetic field and opens when the field is removed. Hall effect sensors on the other hand have no moving parts. These sensors detect the voltage difference (V) that develops on a conductor carrying an electrical current (I) in the presence of a magnetic field (B), see Figure 2.
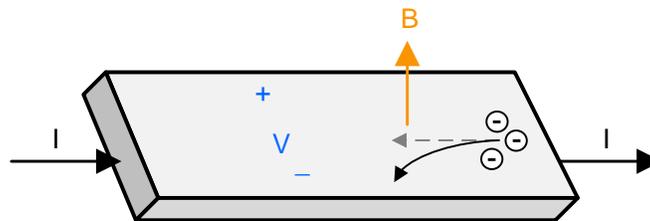
Copyright © 2016, Texas Instruments Incorporated

Figure 2. Simplified Diagram of Hall Effect

The mechanical nature of reed switches limits their lifetime due to the natural wear and tear of the physical switch. The reed switch also suffers from a bounce effect when it opens and closes and can be susceptible to shock and vibration. In contrast, Hall effect sensors do not have any moving parts and, therefore, do not suffer from short lifetimes, do not exhibit bounce effect, and are immune to shock and vibration.

Manufacturing and assembly costs can be also be higher when using reed switches since they must be hand soldered and their glass enclosure can be broken during assembly. In contrast, the small SOT-23 package of the DRV5032 digital Hall effect sensors is more rugged and compact. The DRV5032 can be machined soldered and does not suffer from glass breakage, which lowers manufacturing and assembly costs.

Power consumption can be higher when using a reed switch. Although the reed switch does not consume any power when the switch is open, there will be a small current through a pull-down or pull-up resistor when the switch is closed. The pull-up/pull-down resistor is required to hold the output state when the switch is opened. A 1 MΩ resistor pulled up to 3.0V will draw about 3.0 µA of current when the switch is closed and connected to ground. This current is significant in a battery-powered application. In contrast, the DRV5032FB Hall effect sensor has a push-pull output and does not require a pull-up or pull-down resistor. It's average power consumption in 0.57 µA at 3V and 0.4 µA at 1.8V.

Table 2 summarizes these and other differences between reed switches and Hall effect sensors.

**Table 2. Comparison of Reed Switches and Hall Effect Sensors**

REED SWITCHES	HALL EFFECT SENSOR
Manufacturing issues due to glass breakage, higher manufacturing costs	No glass breakage, lower manufacturing costs
Must be hand soldered, higher assembly cost	Surface mount technology, can be machine-soldered
Bigger form factor	Small package options
Limited life due to mechanical failures	No mechanical parts
Suffer from bounce effect due to shock or vibration	Immune to shock & vibration (no bounce effect), more rugged
Low cost	Low cost
Zero power consumption when open, high power consumption when closed due to required pull-up or pull-down resistor	Low average power (0.4 µA/1.8 V) options available
Simple to use	Simple to use
In-line sensing direction	Perpendicular sensing direction

2.2 Power Supply Design

Because of the increasing battery impedance over the life of the battery supply, it is important to design the power supply network to prevent current spikes generated by the MCU from causing false triggers. While a software algorithm can help to filter such problems, this unwanted power supply feedback loop can become an issue. Ideally, the sensor supply would be regulated to break this loop; however, in this design the extra quiescent current of a regulator would reduce battery life, so other methods were explored.

Figure 3 shows a simplified schematic of the power supply network. The PMOS transistor is used in place of the traditional Schottky diode for reversed battery protection. Because the peak currents are in the 10-mA range when the radio transmits, using a low R_{DS_ON} PMOS provides a much lower voltage drop compared to a Schottky diode, which helps to maximize battery life by allowing the battery to decay to a lower voltage before the circuit is no longer able to function (for more on this technique, see the application report *Reverse Current/Battery Protection Circuits* (SLVA139).

NOTE: The actual design uses two PMOS transistors in series as required by the battery manufacturer to provide added reverse current protection.
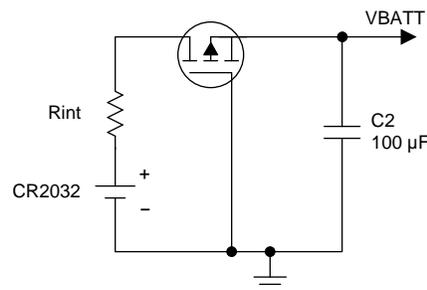
Copyright © 2016, Texas Instruments Incorporated

Figure 3. Simplified Power Supply Network Schematic

Copyright © 2016, Texas Instruments Incorporated

Capacitor C2 supplies the circuit during periods of high and fast peak current demand, which helps to maximize the battery capacity and minimize voltage droop on the power supply rail, especially as the battery approaches its end of life and its internal impedance increases (represented by Rint in Figure 3). The calculation for C2 is provided in Equation 1. For more details on this calculation and the effects of high current peaks on batter life and capacity, see the white paper *Coin cells and peak current draw* (SWRA349).

$$C2 = \frac{\Delta Q}{V_{MAX} - V_{MIN}}$$

(1)

where

- $\Delta Q = Q_{dis} - \frac{V_{MIN}}{Rint} t_{tot}$

- $Q_{dis} = \sum i_n \times t_n$

V_{MAX} is the voltage across the capacitor at the start of the current pulse at the end of the battery's life, and V_{MIN} is the circuit operating minimum. V_{MAX} is taken to be 2.698 V assuming an unloaded end of life battery voltage of 2.7 V (V_P).

Based on the power consumption characterization presented in Section 4.2.1, the TI Design experiences a period of high-current consumption during packet transmit. The load profiles based on a data packet and a poll packet are shown in Figure 17 and Figure 18.

Based on these two profiles, two different values for capacitor C2 can be calculated using Equation 1:

$$C2(Data) = \frac{10.0\,mA \times 29.1\,ms - \frac{2.0\,V}{1\,k\Omega} \times 29.1\,ms}{2.698\,V - 2.0\,V} = 333.5\,\mu C$$

(2)

$$C2(Poll) = \frac{10.0\,mA \times 28.0\,ms - \frac{2.0\,V}{1\,k\Omega} \times 28.0\,ms}{2.698\,V - 2.0\,V} = 321.9\,\mu C$$

(3)

This design uses C2 = 330 μF and additional decades of capacitors in parallel for improved impedance at higher frequencies. The time required to recharge the composite C2 capacitor after the high current event is given in Equation 4.

$$T = Rint \times C2_{comp} \times \ln\left(\frac{V_P - V_{MIN}}{V_P - V_{MAX}}\right) = 1\,k\Omega \times 341.11\,\mu F \times \ln\left(\frac{2.7\,V - 2.0\,V}{2.7\,V - 2.698V}\right) \approx 2.00\,s$$

(4)

Polling packets are periodic, their time interval is fully controlled by firmware. The capacitor will be sufficiently charged to support subsequent polling packets as long as the polling interval exceeds the capacitor charging time. However, data packets are triggered after an event is generated by the Hall effect sensor and, therefore, are asynchronous in nature. Firmware must ensure that data packets are spaced apart sufficiently enough to allow the capacitor to charge.

2.3 Wireless Network Design

This design leverages TI's SimpleLink TI-15.4 Stack to implement a star network. The TI-15.4 Stack implements the standard IEEE 802.15.4e/g specification and is designed to run on SimpleLink CC1310 ultra-low-power MCUs. The TI 15.4 Stack supports different modes including frequency hopping where network devices hop on different frequencies, beacon mode where the network coordinator transmits periodic beacons to indicate its presence, and non-beacon mode where the coordinator does not send out periodic beacons.

The network consists of a central device, or collector, and one or more sensor nodes. The collector performs the functions of a network coordinator (starts the network, allows devices to join the network) and receives data from the sensor nodes. The collector then sends periodic tracking request messages (to which it expects tracking response messages) to determine whether or not the sensor nodes are alive in the network.

Sensor nodes join the network started by the collector. They send sensor data reports to the collector, and respond to the tracking messages sent by the collector. The sensor nodes also poll for messages from the collector allowing for two-way communication. The period of these poll messages can be modified or completely disabled to save power.

This TI Design together with a CC1310 LaunchPad implement the function of a sensor node. The TI-15.4 Stack is configured for operation in the 915-MHz frequency band (frequency hopping disabled), non-beacon mode enabled, and transmit power set to 0 dBm. The polling feature is completely disabled to save power.

2.4   Firmware Control

The sensor firmware connects to the network and processes interrupts from the Hall effect sensors. The firmware will keep the CC1310 standby mode until one of the Hall effect sensors generates an interrupt by toggling its digital output pin. When the CC1310 is woken up by the Hall effect sensor interrupt, it will assemble and send a packet to the collector indicating the status of the Hall effect sensors outputs. A "low" state in the output of the DRV5032FB indicates a magnetic field is present while a "high" state indicates no magnet is present. The CC1310 will return to standby mode until the next interrupt from the Hall effect sensors.

The sensor firmware consists of an application running on top of TI's real-time operating system (TI-RTOS), see Figure 4. TI-RTOS includes the SYS/BIOS kernel, optimized power management, and peripheral drivers. The TI-15.4 Stack runs along side TI-RTOS and handles all network operations. The application services interrupts from the Hall effect sensors and processes commands received from the network.

The serial flash on the LaunchPad can consume a significant amount of power if it is not powered down. The sensor firmware places the serial flash in its powered down mode through a SPI command.
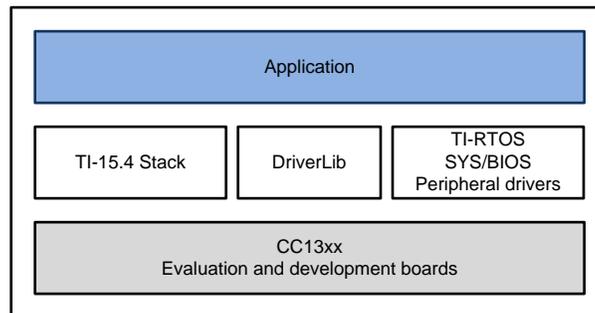
Figure 4. Sensor Firmware Block Diagram

This TI Design allows for the Hall effect sensors to be powered completely from the CC1310 GPIO pins. The sensor firmware always keeps these pins set high. However, duty cycling the power supply pin of the Hall effect sensors can be easily implemented by modifying the application code.

The firmware turns on the TI Design LEDs when the Hall effect sensors detect the presence of a magnet. This feature can be disabled in firmware to save power.

As mentioned in Section 2.3, the sensor firmware can be configured to periodically check for messages from the collector. The period of this polling function is configured through the CONFIG_POLLING_INTERVAL, MIN_POLLING_INTERVAL, and MAX_POLLING_INTERVAL pre-compiler directive in the sensor firmware source code. The feature can be completely disabled by setting CONFIG_POLLING_INTERVAL to zero. Note that the collector firmware also includes a CONFIG_POLLING_INTERVAL pre-compiler directive, which must be set to the same value as the one in the sensor firmware.

3   Getting Started Hardware and Firmware

3.1   Hardware

Figure 5 shows the hardware for the Low-Power Door and Window Sensor With Sub-1GHz and 10-Year Coin Cell Battery Life Reference Design. The printed circuit board (PCB) is in a 34-mm×53-mm rectangular form factor. The Hall effect sensors, several test points, CR2032 battery holder, and jumpers are located on the top side of the PCB.
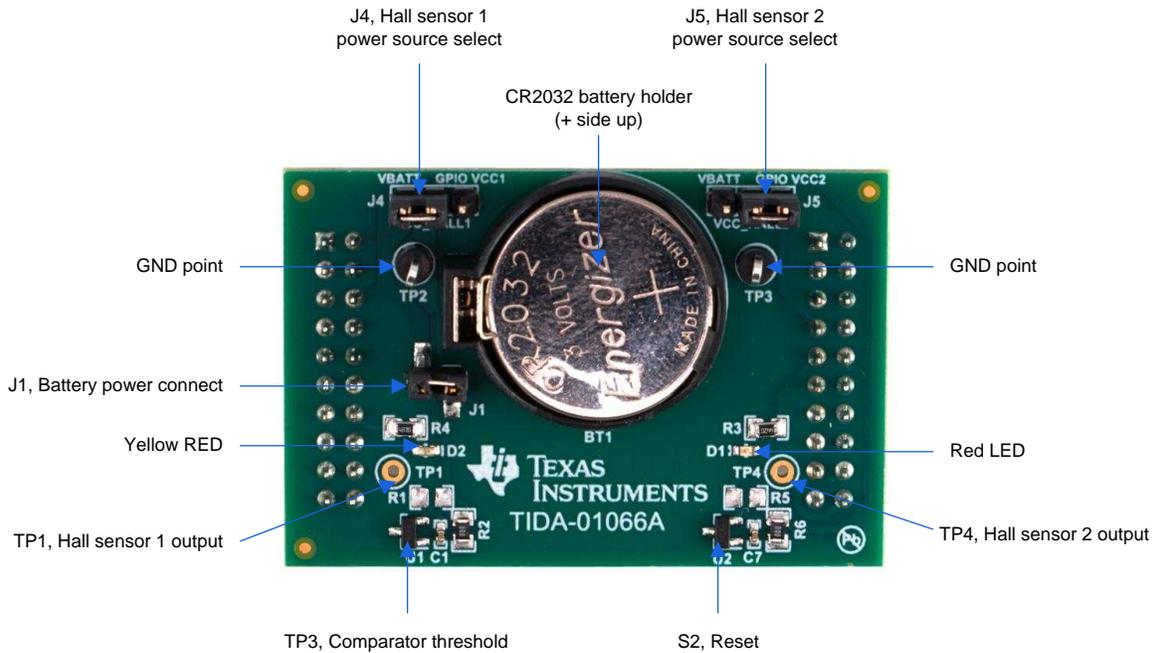

Figure 5. Reference Design Hardware Description

As shown in Figure 6, the TI Design PCB is designed to attach directly to the CC1310 LaunchPad (LAUNCHXL-CC1310). The TI Design PCB and the CC1310 LaunchPad together make up the sensor node. The assembled system can be powered from the USB port on the CC1310 LaunchPad or from the battery on the PCB. SeeSection 3.1.1 for more details on the jumper configuration for each of these two options.

For a complete system, a collector node is required consisting of a second CC1310 LaunchPad and a LCD BoosterPack (http://www.ti.com/tool/430boost-sharp96), see Figure 7.

Figure 6. Fully Assembled System (Sensor Node)   Figure 7. Fully Assembled System (Collector Node)

Table 3 lists the assignments of different signals in the TI Design PCB to the input/output pins of the CC1310 LaunchPad.

Table 3. Pin Assignments When Used with CC1310 LaunchPad

SIGNAL	PIN ASSIGNMENT
HALL2_OUT	DIO15
RLED	DIO18
GPIO_VCC2	DIO19
GPIO_VCC1	DIO25
YLED	DIO29
HALL1_OUT	DIO30

3.1.1 Jumper Configuration

To properly operate the TI Design, the jumpers on the TI Design PCB and the CC1310 LaunchPad must be installed correctly.

To power the entire system from the CC1310 LaunchPad and enable the on-board emulator configure the jumpers as follows:

- TIDA-01066 Board J1 = Opened (disconnects battery from system)
- CC1310 LaunchPad P4 = All jumpers on (XDS110 powers CC1310 and TIDA-01056 Board, all JTAG signals connected to CC1310)
- CC1310 LaunchPad P10: Set to XDS110 Power (full debug supported)
- (Optional) CC1310 LaunchPad P6: Both jumpers on (enables LEDs)

To power the entire system from the coin cell battery and disable the on-board emulator configure the jumpers as follows:

- TIDA-01066 Board J1 = Jumper on (connects battery to system)
- CC1310 LaunchPad P4 = All jumpers removed (removes XDS power from CC1310 and TIDA-01056 Board, disconnects all JTAG signals)
- CC1310 LaunchPad P10: Off (removes power from level shifters, disables debug)
- (Optional) CC1310 LaunchPad P6: Both jumpers removed (disables LEDs)

3.1.2 Test Point Description

This TI Design includes several test points to monitor critical signals. The following is a brief description of these test points:

- TP1: Hall effect sensor 1 digital output
- TP2, TP3: Ground points for probes or common points for voltage measurements
- TP4: Hall effect sensor 2 digital output

3.1.3 Battery Requirements

The battery used in this TI Design must meet the following requirements:

- CR2032 UL certified battery
- Voltage: 3.0 V
- Min capacity: 240 mAh
- Min discharge rate: 0.19 mA

> **NOTE:** Only insert Energizer CR2032VP Lithium battery or equivalent.

> **NOTE:** The battery must be replaced by a trained professional.

3.2   Loading Firmware

Included in the TI Design firmware is a set of pre-built hex images for the collector and the sensor node which can be loaded through the on-board emulator on the CC1310 LaunchPad. The loading procedure is the same for both. Simply configure the jumpers on the CC1310 Launchpad to enable the onboard emulator (see Section 3.1.1) and connect a USB cable to the CC1310 LaunchPad.

After setting up all the hardware, follow these steps to load the firmware on the sensor and collector using the SmartRF Flash Programmer 2:

1. Download and install SmartRF Flash Programmer 2 (http://www.ti.com/tool/flash-programmer).

2. Open SmartRF Flash Programmer 2.

3. In the "Connected devices" window, CC1310 should be listed under XDS110. If it is not listed, check the USB connection to the CC1310 LaunchPad and click "Refresh" button to rescan for devices. Highlight the CC1310 device.

4. In the "Main" tab, click the "Multiple" radio button.

5. **IMPORTANT**: In the "Main" tab, under "Actions", click the "All unprotected pages" radio button. This will erase previous network association information.

6. If loading firmware on the sensor, click on the "Browse" button and navigate to the TIDA-01066 firmware folder and select the TIDA01066_timac_cc13xx_rfd.hex file. Repeat the process to add the TIDA01066_sensor.hex file. See Figure 8.
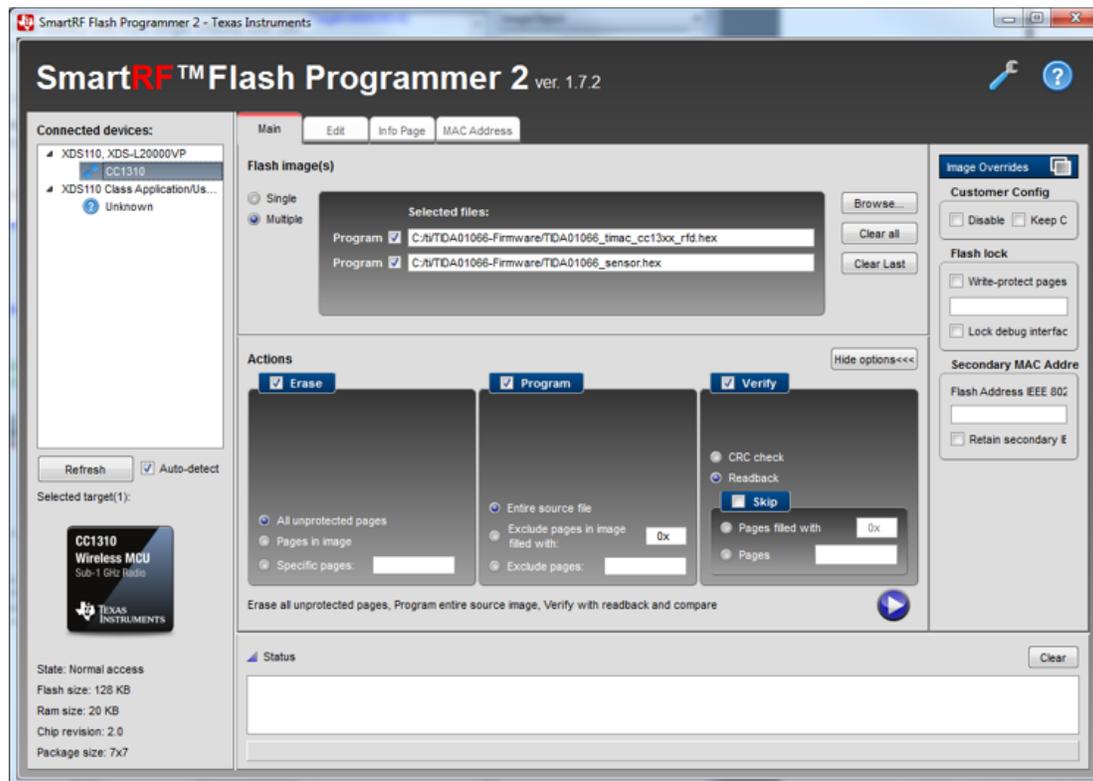
Figure 8. SmartRF Flash Programmer 2 Configuration (Sensor)

7. If loading firmware on the collector, click on the "Browse" button and navigate to the TIDA-01066 firmware folder and select the TIDA01066_timac_cc13xx_ffd.hex file. Repeat the process to add the TIDA01066_collector.hex file. See Figure 9.
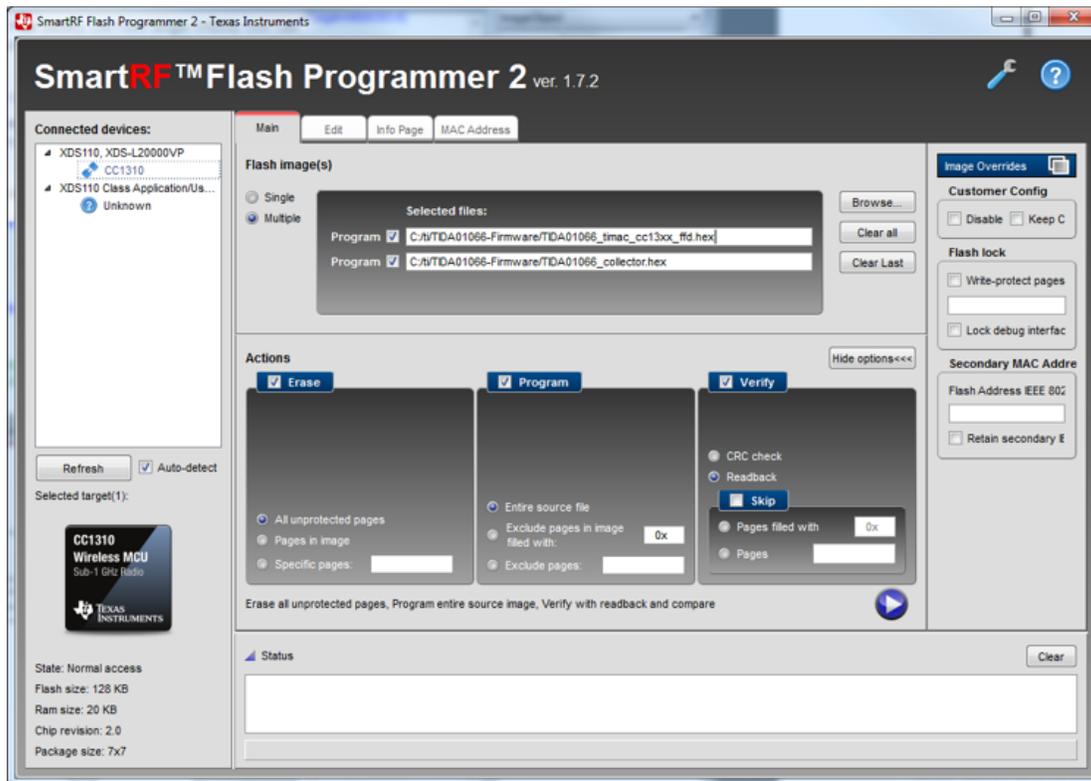
Figure 9. SmartRF Flash Programmer 2 Configuration (Collector)

8. Click on the blue circle play button to flash the firmware image onto the sensor. The status bar on the bottom of SmartRF Flash Programmer 2 will show if flashing the image was successful.

3.3   Starting the Firmware

As described in Section 2.3 and Section 2.4 this TI Design demonstrates a wireless network consisting of a collector and a sensor node. To start the TI-15.4 Stack based network, follow these steps:

1. Set up the collector and sensor node as described in Section 3.1.

2. Power on the collector to start the network. The red LED turns on when network has been started.

3. Press the right button (BTN-2) on the collector to allow new devices to join the network. The red LED blinks when the network is open to new devices.

4. Power on the sensor node. When the sensor has joined the network, the red LED (if enabled) on the sensor LaunchPad is set solid.

The LCD screen on the collector the will display the message shown in Figure 10 after the sensor has successfully joined the network. When a magnet is passed near the Hall effect sensors, the sensor LaunchPad will send a message to the collector indicating the status (open or closed) of a fictional door or window.

Figure 10. Collector Message After Sensor Joins Network
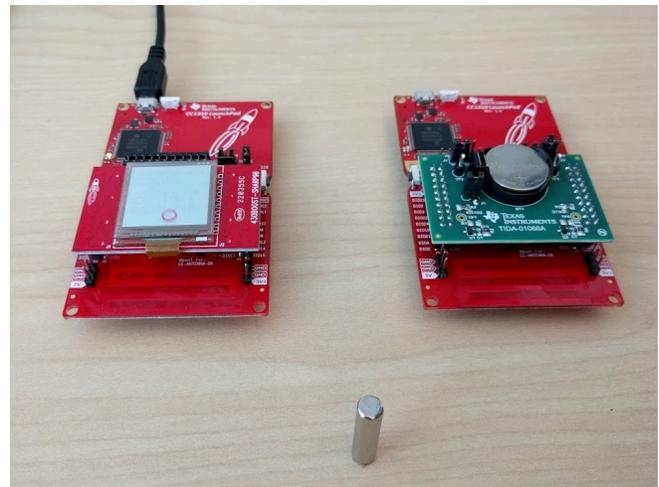
Figure 11. Full Setup Consisting of Collector and Sensor Node

3.4 Building the Firmware

This TI Design includes the full source code for the collector and sensor applications as well as the TI-15.4 Stack. The firmware used on this TI Design was developed using TI's Code Composer Studio™ software (CCS) version 6.1.3. There are three CCS projects in the TI Design firmware installer: one for the sensor, one for the collector, and one for the TI-15.4 Stack.

Follow these steps to setup the CCS projects:

1. Download the TI-15.4 Stack SDK from www.ti.com and follow the installation instructions. Note that the TI Design firmware was developed and tested with version 2.0.0 of the TI-15.4 Stack SDK.
2. Download and install the TI Design firmware.
3. Import the CCS projects into the workspace.
    (a) Select "Import" under the "File" menu.
    (b) Select "CCS Projects" under the "Code Composer Studio" option and click "Next".
    (c) Specify the location of the TI Design CCS project under the "Select archive file" option.
    (d) Click "Finish" to import the files to the CCS workspace.
    (e) Repeat the process for the other CCS projects.
4. Build the collector and sensor CCS project.
    (a) Select the project.
    (b) Select "Build" project from the "Project" menu.
    (c) The TIDA01066_sensor.hex and TIDA01066_collector.hex image files are located under the "sensor_cc1310lp" and the "collector_cc1310LP" folders in their respective projects.
5. Build the TI-15.4 Stack project for the sensor.
    (a) Select the project.
    (b) Select the "Stack-RFD" build configuration from "Project", "Build Configurations", and "Set Active" menu.
    (c) Select "Build" project from the "Project" menu.
    (d) The TIDA01066_timac_cc13xx_rfd.hex image file is located under the "Stack-RFD" folder.
6. Build the TI 15.4-Stack project for the collector.
    (a) Select the project.
    (b) Select the "Stack-FFD" build configuration from "Project", "Build Configurations", and "Set Active" menu.
    (c) The TIDA01066_timac_cc13xx_ffd.hex image file is located under the "Stack-FFD" folder.

NOTE: Follow the steps in the TI-15.4 Stack documentation to set the transmit power for the collector and sensor nodes.

Follow the steps in Section 3.2 to load the hex images on the CC1310 LaunchPads.

4   Testing and Results

4.1   Test Setup

The Low-Power Door and Window Sensor With Sub-1GHz and 10-Year Coin Cell Battery Life Reference Design has been characterized to support all of the critical specifications for this subsystem. The following sections describe the test setups for these measurements including the equipment used and the test conditions unless otherwise noted.

4.1.1   Power Consumption

The power consumption measurements for this reference design were critical in estimating battery life. Measurements of supply current were performed on the reference design hardware.

The majority of the time, the system will operate in a very low-power consumption state, often only consuming microamps of current. The test setup for measuring these small currents is illustrated in Figure 12.

The resolution setting of the Agilent 34411A 6½ digit multimeter can place a limit on the amount of instantaneous current flowing to the DUT. This can become a problem since at different points during normal operation the current will jump from the microamp range to the milliamp range. For example, when powering on the board, there will be an initial inrush of current to the board. Generally, a resolution of 10 mA is enough to prevent any issues with current limits.
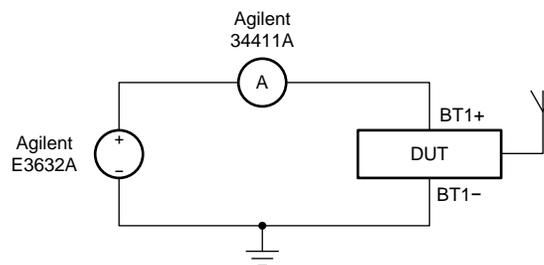
Copyright © 2016, Texas Instruments Incorporated

Figure 12. Test Circuit Used for Measuring Small Currents

The system will also experience peaks of high current such as those generated during radio transmission. The measurement of these intervals involves using a current probe that interfaces to an oscilloscope, which can then be used to trigger on the high current events. This setup is illustrated in Figure 13.
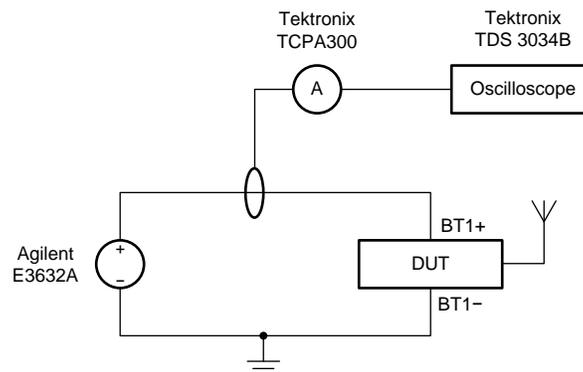
Copyright © 2016, Texas Instruments Incorporated

Figure 13. Test Circuit Used for Measuring Supply Current During High-Peak Currents

Copyright © 2016, Texas Instruments Incorporated

4.1.2 Magnet Response

The sensing range of the DRV5032FB was tested using two Neodymium-N42 magnets with different dimensions and strengths. Table 4 provides specific information on the magnets which were used for testing. Figure 14 and Figure 15 show photographs of the small and large magnets.

The magnets were brought close to each sensor on the TI Design. Different directions and orientations were tested. Firmware running on the CC1310 LaunchPad was modified to toggle the red and yellow LEDs on the TI Design as soon as the Hall effect sensor switched its output. The approximate distances at which the sensor triggered were recorded.

Table 4. Magnets Used for Testing

PART NUMBER	MANUFACTURER	DIMENSIONS	TYPE	GRADE	SURFACE FIELD	DESCRIPTION
D4E	K&J Magnetics	¼" dia. × 7/8" length/thick	Neodymium	N42	6534 Gauss	Small cylindrical magnet
DCX0	K&J Magnetics	¾" dia. × 1" length/thick	Neodymium	N42	6180 Gauss	Large cylindrical magnet

Figure 14. Small Cylindrical Magnet (D4E)

Figure 15. Large Cylindrical Magnet (DCX0)

4.1.3 Wireless Range

The range of the wireless sub-1GHz RF was measured using two CC1310 LaunchPads. One CC1310 LaunchPad was setup as a collector as described in Section 3.3, and the other was fitted with the Low-Power Door and Window Sensor With Sub-1GHz and 10-Year Coin Cell Battery Life Reference Design. For this test, the collector LaunchPad remained at a stationary location as the sensor LaunchPad was moved away. While the sensor LaunchPad was on the move, a magnet was continuously passed in front of the Hall effect sensor to make sure there were radio packets constantly being transmitted. The distance at which packets were no longer received was then measured.

4.2 Test Data

> **NOTE:** Unless otherwise noted, the test data in the following sections were measured with the system at room temperature. All of the measurements in this section were measured with calibrated lab equipment.

4.2.1 Power Characterization

Because the primary purpose of this TI Design is to showcase a battery-powered wireless sensor, characterization of the system's power consumption is critical.

This TI Design will remain primarily in the standby state, which is the default state when the no change in the magnetic field is detected. It is critical that the power consumption of this state remain as low as possible such that the battery life of the system can be maximized. In this state, the CC1310 will receive power, but will go into its standby mode to minimize power consumption. The DRV5032FB Hall effect sensors will remain active and continuously monitor the magnetic field.

Table 5 and Figure 16 show the average current consumption of the entire system when it is operating in the standby mode. The current consumption was characterized across different battery voltages. As expected, the current consumption increases at the lower voltage ranges since the internal DC-DC of the CC1310 must recharge the bypass capacitors more often to maintain a constant supply voltage. For battery life calculations, the average current was calculated over the range of battery voltages from 3.3 V to 2.4 V. The average current for standby mode in these voltage ranges is *1.97 µA*.

Table 5. Average Current Consumption Across Battery Voltage in Standby Mode

VBATT (V)	AVERAGE SYSTEM CURRENT (A)		
	RUN 1	RUN 2	RUN 3
3.80	2.06E-6	2.02E-6	2.20E-6
3.60	2.04E-6	2.04E-6	2.00E-6
3.30	2.00E-6	2.02E-6	1.99E-6
3.00	2.09E-6	2.06E-6	2.00E-6
2.80	1.93E-6	1.92E-6	1.96E-6
2.60	1.83E-6	1.89E-6	1.89E-6
2.40	1.93E-6	2.11E-6	2.00E-6
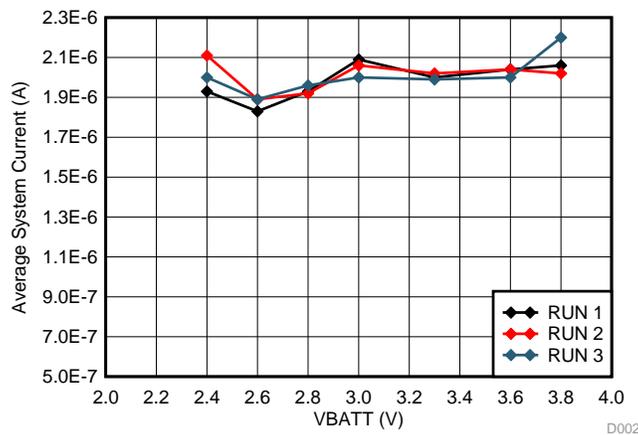
Figure 16. Average Current Consumption Across Battery Voltage in Standby Mode

When a change in the magnetic field is detected, the Hall effect sensor will trigger an wake-up interrupt to the CC1310. The CC1310 will read the output of the Hall effect sensors and transmit a packet to the collector device. The CC1310 will return to the standby state until the next interrupt is received from the Hall effect sensors. Transmitting a packet is the most power-consuming function of the system. Figure 17 captures the high-current consumption due to the transmission of a packet after an event is triggered by the Hall effect sensor. The average current consumption was *7.70 mA* over a total duration of *29.1 ms*.

Δ: 300µA
@:   500µA

Δ: 29.1ms
@:   23.2ms

Ch4 Mean
7.70mA

M 4.00ms   A   Ch4 � 8.90mA

Ch4 5.00mAΩ

T 28.00 %

13 Sep 2016
13:27:25
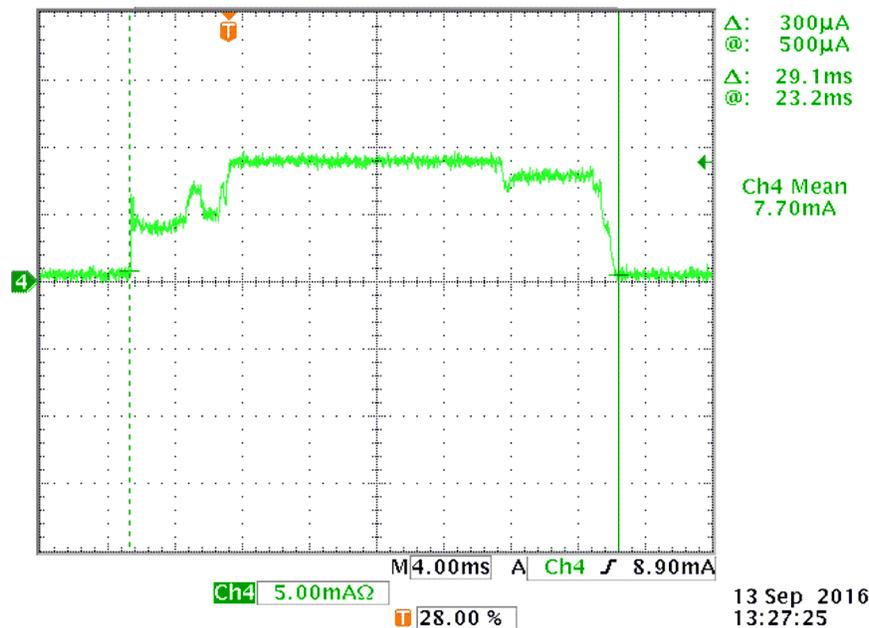
Figure 17. Wireless Packet Transmit Current Due To Hall Effect Sensor Event

The TI-15.4 Stack allows for the collector to send messages to the sensor at a period specified by the collector. The sensor will automatically wake-up and poll for these messages. The polling frequency as well as the number of packets transmitted is dependant on the application requirements. Since the sensor must periodically wake-up to check for messages from the collector, using a longer polling period will result in longer battery lifetimes. Figure 18 captures the high-current consumption due to the transmission of a packet after a polling event. Note that in this case, there is no data sent back by the collector; back-and-forth communication between the sensor and collector will increase current consumption. For the purposes of this TI Design, it was assumed that the majority of the time, there would be no data sent from the collector to the sensor node. The average current consumption was *6.23 mA* over a total duration of *21.1 ms*.

Δ: 0.00 A
@:   200µA

Δ: 21.1ms
@:   −20.8ms

Ch4 Mean
6.23mA

M 4.00ms   Width   Ch4

Ch4 5.00mAΩ

T 73.60 %

13 Sep 2016
13:45:41
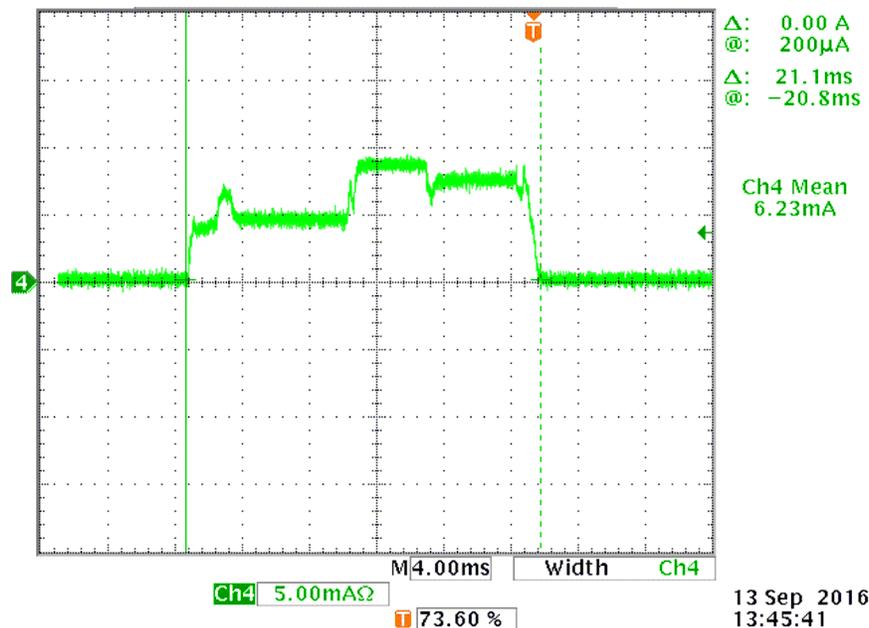
Figure 18. Wireless Packet Transmit Current Due To Polling Event

4.2.1.1 *Battery Life Calculations*

The main parameters that affect the estimated battery life of the entire system are:

- Capacity rating of the battery in milliamp-hours (mAh)
- Average standby-state current consumption (µA)
- Standby-state duration (s)
- Average packet current consumption (mA)
- Packet transmission duration (ms)
- Polling rate

Equation 5 describes the estimated battery life of the system:

$$\text{Battery Lifetime}\left(\text{yr}\right) = \frac{\text{Battery Capacity}\left(\text{mAh}\right)}{\left(\dfrac{I_{\text{Standby}}\left(\mu A\right) \times t_{\text{Standby}}\left(s\right) + I_{\text{Data}}\left(\mu A\right) \times t_{\text{Data}}\left(s\right) + I_{\text{Poll}}\left(\mu A\right) \times t_{\text{Poll}}\left(s\right)}{t_{\text{Total}}\left(s\right)}\right)} \times \frac{1\,\text{year}}{8760\,\text{hours}} \times \text{Derating Factor}$$

(5)

In Equation 5 t_{Total} is an arbitrary time interval, t_{Data} is the amount of time spent transmitting data packets, and t_{Poll} is the amount of time transmitting poll packets. If t_{Total} is set equal to the polling interval, then t_{Poll} equals the time it takes to send a single poll packet, 21.1 ms, and the value for t_{Data} is calculated as:

$$t_{\text{Data}} = n\left(\frac{\text{Events}}{\text{hr}}\right) \times \frac{1\,\text{hr}}{3600\,\text{sec}} \times t_{\text{Total}} \times t_{\text{DataPkt}}\left(\text{ms}\right)$$

(6)

In Equation 6 *n* is the number of Hall effect sensor events per hour and t_{DataPkt} is the amount of time it takes to send one data packet, 29.1 ms.

The number of Hall effect sensor events per hour depends entirely on the end-use case. However, for the purpose of this TI Design, the following use-case was defined:

- Door installation
- 48 entries per 24-hour period
- 2 events per entry

Using these requirements, the t_{Data} can be calculated as follows:

$$t_{\text{Data}} = 4\left(\frac{\text{Events}}{\text{hr}}\right) \times \frac{1\,\text{hr}}{3600\,\text{sec}} \times 29.1\,\text{ms} \times t_{\text{Total}} = 32.3 \times 10^{-6} \times t_{\text{Total}}$$

If polling is completely disabled or, alternatively, if the polling interval is set to a very large number, for example, 1×10^6 seconds, the battery life can be estimated as follows:

$$\text{Battery Lifetime}\left(\text{yr}\right) = \frac{240\,\text{mAh}}{\left(\dfrac{1.97\,\mu A \times \left(1 \times 10^6\,s\right) + 7.70\,\text{mA} \times 32.3 + 6.23\,\text{mA} \times 21.1\,\text{ms}}{1 \times 10^6\,s}\right)} \times \frac{1\,\text{year}}{8760\,\text{hours}} \times .85 = 10.5\,\text{years}$$

Table 6 and Figure 19 show the battery life estimates for polling intervals from 1 minute to 1 hour.

Table 6. Battery Lifetime versus Polling Interval

T$_{Poll}$ (min)	I$_{Standby}$ (A)	t$_{Standby}$ (s)	I$_{Poll}$ (A)	t$_{Poll}$ (s)	I$_{Data}$ (A)	t$_{Data}$ (s)	I$_{Avg}$ (A)	BattCap (Ah)	DERATING	BATTERY LIFE (yrs)
1.0E+0	1.97E-6	59.98E+0	6.23E-3	21.10E-3	7.70E-3	1.94E-3	4.41E-6	240.0E-3	0.85	5.28
2.0E+0	1.97E-6	119.98E+0	6.23E-3	21.10E-3	7.70E-3	3.88E-3	3.31E-6	240.0E-3	0.85	7.03
5.0E+0	1.97E-6	299.97E+0	6.23E-3	21.10E-3	7.70E-3	9.70E-3	2.66E-6	240.0E-3	0.85	8.76
10.0E+0	1.97E-6	599.96E+0	6.23E-3	21.10E-3	7.70E-3	19.40E-3	2.44E-6	240.0E-3	0.85	9.55
20.0E+0	1.97E-6	1.20E+3	6.23E-3	21.10E-3	7.70E-3	38.80E-3	2.33E-6	240.0E-3	0.85	10.00
21.0E+0	1.97E-6	1.26E+3	6.23E-3	21.10E-3	7.70E-3	40.74E-3	2.32E-6	240.0E-3	0.85	10.02
24.0E+0	1.97E-6	1.44E+3	6.23E-3	21.10E-3	7.70E-3	46.56E-3	2.31E-6	240.0E-3	0.85	10.08
27.0E+0	1.97E-6	1.62E+3	6.23E-3	21.10E-3	7.70E-3	52.38E-3	2.30E-6	240.0E-3	0.85	10.12
30.0E+0	1.97E-6	1.80E+3	6.23E-3	21.10E-3	7.70E-3	58.20E-3	2.29E-6	240.0E-3	0.85	10.16
33.0E+0	1.97E-6	1.98E+3	6.23E-3	21.10E-3	7.70E-3	64.02E-3	2.29E-6	240.0E-3	0.85	10.19
36.0E+0	1.97E-6	2.16E+3	6.23E-3	21.10E-3	7.70E-3	69.84E-3	2.28E-6	240.0E-3	0.85	10.22
39.0E+0	1.97E-6	2.34E+3	6.23E-3	21.10E-3	7.70E-3	75.66E-3	2.28E-6	240.0E-3	0.85	10.24
42.0E+0	1.97E-6	2.52E+3	6.23E-3	21.10E-3	7.70E-3	81.48E-3	2.27E-6	240.0E-3	0.85	10.25
45.0E+0	1.97E-6	2.70E+3	6.23E-3	21.10E-3	7.70E-3	87.30E-3	2.27E-6	240.0E-3	0.85	10.27
48.0E+0	1.97E-6	2.88E+3	6.23E-3	21.10E-3	7.70E-3	93.12E-3	2.26E-6	240.0E-3	0.85	10.28
51.0E+0	1.97E-6	3.06E+3	6.23E-3	21.10E-3	7.70E-3	98.94E-3	2.26E-6	240.0E-3	0.85	10.30
54.0E+0	1.97E-6	3.24E+3	6.23E-3	21.10E-3	7.70E-3	104.76E-3	2.26E-6	240.0E-3	0.85	10.31
57.0E+0	1.97E-6	3.42E+3	6.23E-3	21.10E-3	7.70E-3	110.58E-3	2.26E-6	240.0E-3	0.85	10.32
60.0E+0	1.97E-6	3.60E+3	6.23E-3	21.10E-3	7.70E-3	116.40E-3	2.26E-6	240.0E-3	0.85	10.33
16.7E+3	1.97E-6	999.97E+3	6.23E-3	21.10E-3	7.70E-3	32.33E+0	2.22E-6	240.0E-3	0.85	10.49
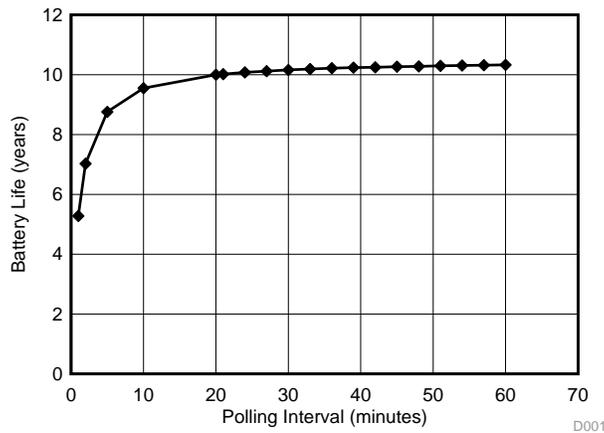
Figure 19. Battery Lifetime versus Polling Interval

24 *Low-Power Door and Window Sensor With Sub-1GHz and 10-Year Coin Cell Battery Life Reference Design* TIDUC69–September 2016

Submit Documentation Feedback

4.2.2 Magnet Response

The magnet was placed on top of the sensor, with the north-south pole oriented in the z-direction of an imaginary 3D plane, and the sensor laying in the x-y plane, see Figure 20 and Figure 21. The magnet was brought closer to the sensor until the magnetic field became strong enough to trigger the sensor. The results of these tests are summarized in Table 7.
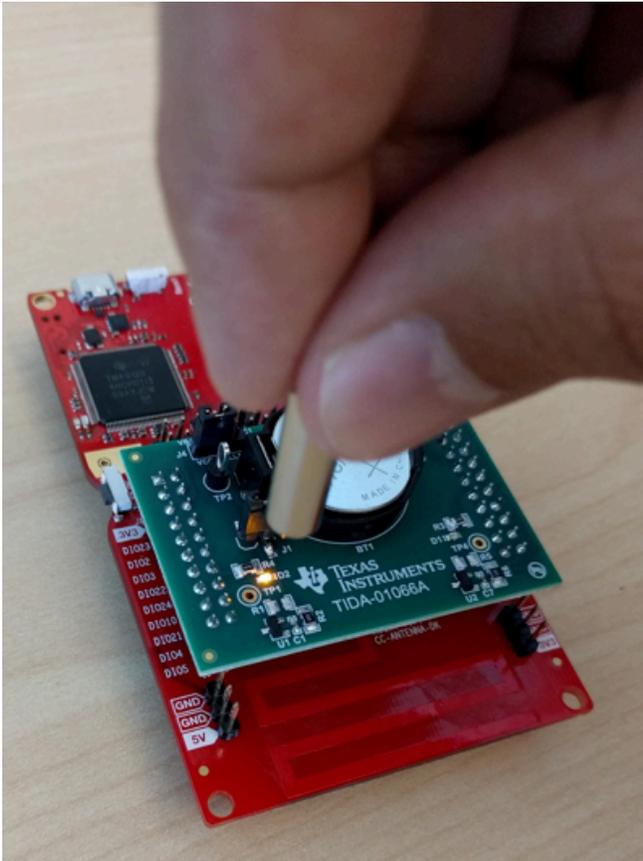
Figure 20. Magnet Top Test Setup (D4E)   **Figure 21. Magnet Top Test Setup (DCX0)**

Table 7. Switching Distance For Magnet Directly On Top of Sensor

MAGNET PART NUMBER	SENSOR	SIMULATED SWITCHING DISTANCE (mm)[1]	MEASURED SWITCHING DISTANCE (mm)
D4E (Small cylindrical magnet)	DRV5032FB	23 to 37	23
DCX0 (Large cylindrical magnet)	DRV5032FB	56 to 89	60

[1] Estimated using online magnetic field calculator and B_{OP} specs in DRV5032 datasheet.

The large magnet was placed on the side of the sensor, with the north-south pole oriented in the z-direction of an imaginary 3D plane, and the sensor laying on the x-y plane, see Figure 22. The magnet was brought closer to the sensor until the magnetic field became strong enough to trigger the sensor. The tampering sensor was able to detect the magnet up at about 30 mm.
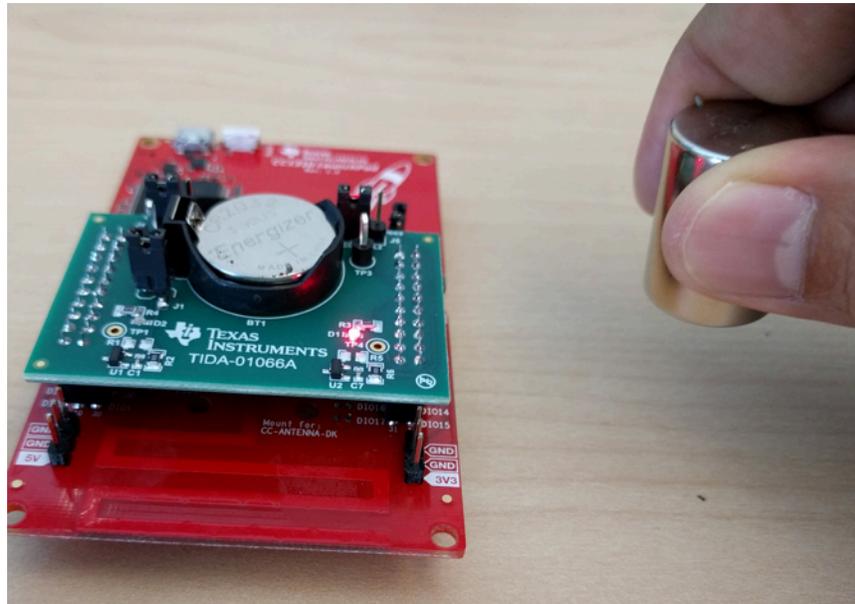
Figure 22. Magnet Side Test Setup (DCX0)

The shape, size, and material composition of the magnet will have yield different results from those mentioned above. Various magnetic field calculators are available online, which allows the user to simulate strength of the magnetic field at different distances for magnet of a user-defined shape, size, and type. Using the BOP specs in the Hall effect sensor datasheet, the switching distance can be calculated. The TI Design hardware can accommodate various DRV part numbers for easy prototyping.

4.2.3   Wireless RF Range

The wireless RF range was measured to be approximately 60 meters in a typical office environment with direct line of sight.

There are ways to increase this distance even further. Use of a whip antenna with gain instead of the passive PCB antenna could offer improvements in the wireless RF range. Another option would be to increase the transmit power of the CC1310 at the expense of increased supply current during the radio transmission intervals.

5 Design Files

5.1 Schematics

To download the schematics for the board, see the design files at TIDA-01066.

5.2 Bill of Materials

To download the bill of materials (BOM), see the design files at TIDA-01066.

5.3 PCB Layout Recommendations

The Low-Power Door and Window Sensor With Sub-1GHz and 10-Year Coin Cell Battery Life Reference Design was laid out using a two-layer PCB. The top and bottom layers are used for general signal routing and also have GND fills in unused areas. For all of the TI products used in this TI Design, adhere to the layout guidelines detailed in their respective datasheets.

5.3.1 Layout Prints

To download the layer plots, see the design files at TIDA-01066.

5.4 Altium Project

To download the Altium project files, see the design files at TIDA-01066.

5.5 Gerber Files

To download the Gerber files, see the design files at TIDA-01066.

5.6 Assembly Drawings

To download the assembly drawings, see the design files at TIDA-01066.

6 Software Files

To download the software files, see the design files at TIDA-01066.

7 References

1. Texas Instruments, *Reverse Current/Battery Protection Circuits*, Application Report (SLVA139)
2. Texas Instruments, *Coin Cells and Peak Current Draw*, WP001 White Paper (SWRA349)

8 About the Author

CHRISTINA S. LAM is a systems architect at Texas Instruments, where she is responsible for developing firmware for reference design solutions in the industrial segment. Christina has broad experience with applications processors, microcontrollers, and digital-signal processors with specialties in embedded firmware. Christina earned her bachelor of science (BS) in electrical and computer engineering from the University of Texas at Austin.

GUSTAVO MARTINEZ is a senior systems architect at Texas Instruments where he is responsible for developing reference designs for industrial applications. Gustavo has ample experience developing system reference designs for the Smart Grid and home automation segments, which include high performance application processors, floating-point digital signal processors, and RF technology. Gustavo obtained his master of electrical engineering degree from the University of Houston and his bachelor of science in electrical engineering degree from the University of Texas at El Paso.